Asymptotic solution of transonic nozzle flows with homogeneous condensation. II. Supercritical flows

Can F. Delale, Günter H. Schnerr, and Jürgen Zierep

Asymptotic solution of transonic nozzle flows with homogeneous condensation. II. Supercritical flows

Can F. Delale,[a),b)] Günter H. Schnerr, and Jürgen Zierep
Institut für Strömungslehre und Strömungsmaschinen, Universität (TH) Karlsruhe, Germany

(Received 3 August 1992; accepted 7 June 1993)

A detailed analysis of supercritical transonic nozzle flows with stationary normal shock waves is presented. A classification scheme based on the normal shock location is obtained using asymptotic methods, and four distinct supercritical flow regimes are distinguished. A simple shock fitting technique that determines the shock location within any desired precision is introduced. Consequently, an algorithm that exhibits the asymptotic solution in each supercritical flow regime is developed for the expansion of moist air in nozzles with atmospheric supply conditions by utilizing the classical nucleation theory and the Hertz–Knudsen droplet growth law. Good agreement with the recent static pressure measurements and visualized shock locations is achieved in relatively slender nozzles when the condensed phase is assumed to consist purely of water drops.

I. INTRODUCTION

The asymptotic solution of transonic nozzle flows with heat addition from nonequilibrium homogeneous condensation presented in the previous paper,[1] which will be referred to as Paper I in this paper, is valid only for subcritical or smooth flows, where the amount of heat released does not exceed a critical value. If with the same working fluid and nozzle geometry and for fixed initial specific humidity and fixed reservoir temperature, the initial relative humidity is increased beyond a certain limit, then the amount of heat released by condensation may exceed the critical amount. In such a case the effect of heat release outweighs the influence of increasing cross section, moving the flow Mach number (the Mach number based on the local frozen speed of sound) toward unity. The flow is then said to be "thermally choked" and the inclusion of a stationary normal shock wave becomes necessary. Such flows will be termed supercritical, in contrast to subcritical or smooth flows. If the initial relative humidity is further increased with the rest of the conditions kept fixed, the normal shock becomes unstable, and an unsteady periodic flow pattern sets in near the throat.

Supercritical nozzle flows with stationary normal shock waves formed by excessive heat release from given internal heat source distributions were first considered by Jungclaus and van Raay,[2] and a comprehensive treatment of the subject can be found in Zierep.[3] Early investigations of supercritical nozzle flows with heat addition from nonequilibrium condensation were made by Pouring,[4] Barschdorff,[5] and Barschdorff and Fillipov,[6] and a simplified asymptotic analysis has recently been carried out by Clarke and Delale.[7]

Pouring considers the case of a thermally choked flow with a stationary normal shock in moist air expansions through a converging–diverging Laval nozzle, where he assumes that the pressure distribution is known *a priori* (e.g., empirically). Barschdorff uses an iterative numerical scheme for the solution of the differential equations describing nozzle flows with nonequilibrium condensation of wet steam, where he replaces the singularities by normal shocks with continuous downstream acceleration to supersonic flow. He concludes that condensation of wet steam with a stationary normal shock occurs closer to the throat than the shock-free condensation. Moreover, when the vapor is nearly saturated in the reservoir, he reports that no stationary position for the shock can be found, and that consequently an unsteady periodic flow sets in (unsteady periodic flows in condensing nozzle flows were first observed by Schmidt[8] and Barschdorff[9] and discussed by Mosnier[10] and Wegener and Mosnier[11]). Barschdorff and Fillipov also consider unsteady periodic nozzle flows with condensation and by an approximate analysis arrive at a formula for the frequency of such flows. On the other hand, Clarke and Delale present a simplified asymptotic analysis of supercritical flows with a stationary normal shock wave embedded in the droplet growth zone.

The aim of this paper is to give a detailed analysis of supercritical flows with stationary normal shock waves by extending the asymptotic theory of Paper I. For this reason a brief summary of the theory of thermal choking recently developed by the present authors[12] is first presented. The condensation rate equation is then reconsidered to account for the inclusion of a normal shock wave arising from compressive effects due to excessive heat released by condensation. A classification scheme that leads to four distinct supercritical regimes with stationary normal shock waves is introduced, and the asymptotic solution of the flow field in each regime is presented. The normal shock relations and shock strength are exhibited, allowing for the temperature dependence of the latent heat. A simple shock fitting technique based on accelerating the flow downstream of the shock back to supersonic speeds is introduced. Consequently, an algorithm that utilizes the classical nucleation theory and the Hertz–Knudsen droplet growth law, together with the liquid and ice models of Paper I, is devel-

[a)]Alexander von Humboldt Fellow.
[b)]Permanent address: Department of Mathematics, Bilkent University, Ankara, Turkey.

 0899-8213/93/5(11)/2982/14/$6.00

oped for moist air expansions under atmospheric supply conditions. Good agreement with the recent static pressure measurements and with the visualized shock locations by Schnerr[13] is achieved when the liquid model for the condensed phase is employed in relatively slender nozzles.

Only supercritical flows with stationary normal shock waves are considered in this paper. Also worth mentioning is that the notation used in this paper follows precisely that of Paper I.

II. THERMAL CHOKING

In this section we present a brief account of the theory of thermal choking recently developed by Delale *et al.*[12] For this reason we first write Eq. (9) of Paper I conveniently in the form

$$\Delta(g,x)=T_0\Theta(g)\left(\frac{q^*(g,x)}{c_{p0}T_0}-\frac{q(g,x)}{c_{p0}T_0}\right), \tag{1}$$

where $q(g,x)/(c_{p0}T_0)$ denotes the amount of heat released by condensation up to a location x, given by

$$\frac{q(g,x)}{c_{p0}T_0}=\frac{gL}{c_{p0}T_0}, \tag{2}$$

$q^*(g,x)/(c_{p0}T_0)$ is the critical amount of heat defined by

$$\frac{q^*(g,x)}{c_{p0}T_0}\equiv\frac{\{[1+u_s^2+R(g,x)]/[2u_s]\}^2}{T_0\Theta(g)}-1, \tag{3}$$

and where $\Theta(g)$ is defined by

$$\Theta(g)\equiv\frac{[1+\gamma+(\gamma-1)H^{-1}g][1-H^{-1}g]}{2\gamma}. \tag{4}$$

Naturally $\Delta=0$ [or equivalently, $q(g,x)/(c_{p0}T_0)=q^*(g,x)/(c_{p0}T_0)$] is a necessary condition for a flow to be thermally choked. We call a flow *subcritical* if $\Delta>0$ [or equivalently $q(g,x)/(c_{p0}T_0)<q^*(g,x)/(c_{p0}T_0)$] for all $x>0$, and *supercritical* if $\Delta<0$ [or equivalently $q(g,x)/(c_{p0}T_0)>q^*(g,x)/(c_{p0}T_0)$] for some $x>0$. The necessary and sufficient conditions for the existence of supercritical flows are exhibited in Delale *et al.*,[12] where it is shown in detail how such flows are realized by the existence of normal shock waves due to excessive heat release from condensation. For given nozzle geometry and working fluid these normal shock waves can be stationary (steady flow) or oscillating (unsteady periodic flow) depending on the initial relative humidity for fixed reservoir temperature and fixed initial specific humidity. In what follows we present a detailed asymptotic analysis of supercritical flows with stationary normal shock waves.

III. THE CONDENSATION RATE EQUATION IN SUPERCRITICAL FLOWS

Herein, we reformulate the condensation rate equation for $g(x)$ in the supercritical regime and exhibit the normal shock relation for dg/dx. The reconsideration of the condensation rate equation for supercritical flows is necessary because the structure of the physically distinct condensation zones exhibited for subcritical flows in Paper I alters significantly downstream of the normal shock, depending on its location. Since the location of the normal shock, hereafter denoted by the normalized axial coordinate z, is not known *a priori* (shock fitting), it is essential that the choice for general consideration be made to allow for the most compatible physical phenomena to occur. It is well known that the location of the shock lies downstream of the onset point x_k ($z>x_k$), where, in general, both nucleation and droplet growth are important. Thus, without loss of generality we assume that nuclei production continues downstream of the normal shock no matter how short this period can take. The limiting case where nucleation has completely ceased prior to the shock location can then be determined by simply taking the appropriate limit.

In reformulating the condensation rate equation we first notice that the thermodynamic functions r^*, B, Σ, and Ω of Paper I were taken to be at least piecewise smooth functions of the three independent thermodynamic coordinates: p, T, and g. Across the normal shock, the pressure p and the temperature T are discontinuous. Consequently, the thermodynamic functions r^*, B, Σ, Ω, and the latent heat L of Paper I also exhibit discontinuities across the normal shock location. For notational convenience we reserve subscript 1 for all thermodynamic functions with domain $x\leqslant z$ and subscript 2 for those with domain $x\geqslant z$. Furthermore, we use subscript $(+)$ to denote the variables as $x\to z^+$ and subscript $(-)$ to denote the variables as $x\to z^-$ [e.g., $B_-=\lim_{x\to z^-}B(x)=B_1(z)$, $B_+=\lim_{x\to z^+}B(x)=B_2(z)$, etc.; notice that since B is discontinuous at $x=z$, $B_-\neq B_+$]. The condensation rate equation given in Paper I by Eq. (16), namely,

$$g_1(x)=\int_{x_s}^{x}\left(r_1^*(\xi)+\lambda\int_{\xi}^{x}\Omega_1(\eta)d\eta\right)^3\Sigma_1(\xi)A(\xi)\times\exp[-K^{-1}B_1(\xi)]d\xi, \tag{5}$$

is now valid only upstream of and at the shock location ($x\leqslant z$). Downstream of the shock location ($x>z$) the condensation rate equation can be constructed in a similar fashion, but now taking into account the contribution from downstream nuclei production as well to yield

$$\begin{aligned}g_2(x)=&\int_{x_s}^{z}\left(r_1^*(\xi)+\lambda\int_{\xi}^{z}\Omega_1(\eta)d\eta+\lambda\int_{z}^{x}\Omega_2(\eta)d\eta\right)^3\\&\times\Sigma_1(\xi)A(\xi)\exp[-K^{-1}B_1(\xi)]d\xi\\&+\int_{z}^{x}\left(r_2^*(\xi)+\lambda\int_{\xi}^{x}\Omega_2(\eta)d\eta\right)^3\\&\times\Sigma_2(\xi)A(\xi)\exp[-K^{-1}B_2(\xi)]d\xi.\end{aligned} \tag{6}$$

In Eq. (6) the first integral characterizes the contribution from nuclei created upstream of the normal shock, whereas the second integral characterizes the contribution from nuclei produced downstream of the normal shock. It can easily be demonstrated from Eqs. (5) and (6) that $g(x)$ is continuous, but not differentiable at $x=z$. The continuity of $g(x)$ at $x=z$ is a consequence of the assumption that the droplets pass through the shock unaltered. Differentiating

Eqs. (5) and (6) and taking, respectively, the limits as $x \to z^-$ and $x \to z^+$, we arrive at the normal shock relation for dg/dx:

$$\left(\frac{dg}{dx}\right)_+ = \frac{\Omega_+}{\Omega_-}\left(\frac{dg}{dx}\right)_- + r_+^{*3}\Sigma_+ A_z \exp(-K^{-1}B_+)$$

$$-\frac{\Omega_+}{\Omega_-} r_-^{*3}\Sigma_- A_z \exp(-K^{-1}B_-), \tag{7}$$

where $A_z \equiv A(z) = A_+ = A_-$. In the limit where the normal shock wave is embedded in the droplet growth zone with vanishing nucleation rate, i.e., in the limit as $B_+ = B_- \to \infty$, we obtain the limiting normal shock relation,

$$\left(\frac{dg}{dx}\right)_+ = \frac{\Omega_+}{\Omega_-}\left(\frac{dg}{dx}\right)_- . \tag{8}$$

IV. CLASSIFICATION SCHEME AND ASYMPTOTIC ANALYSIS OF THE RATE EQUATION IN SUPERCRITICAL FLOWS

In this section we present a detailed analysis of supercritical flows. It is well known that when the initial relative humidity of a given working fluid for a given nozzle is gradually increased keeping the initial specific humidity and the reservoir temperature fixed, the onset point x_k shifts toward the throat of the nozzle. In particular, in cases where the initial relative humidity exceeds a certain limiting value with the rest of the conditions kept fixed, the flow becomes thermally choked and normal shock waves occur following the onset of condensation due to compressive effects from excessive heat release by condensation. These normal shock waves are generally embedded in condensation zones where both nucleation and droplet growth are important (in some limiting situations they may be embedded in the droplet growth zone DGZ, where nucleation has completely ceased). The downstream solution following the normal shock location may then alter considerably depending on the zone where the normal shock is embedded. Thus different supercritical flow regimes arise depending on the location of the normal shock.

A. Classification scheme for supercritical flows

In supercritical flows the normal shock may be embedded in any of the zones FGZ (further growth zone), RGZ (rapid growth zone), NZ (nucleation zone with growth), or DGZ (droplet growth zone) of Paper I. In each case the nature and structure of the condensation zones of Paper I alter considerably downstream of the normal shock.

Figures 1(a)–1(d) distinguish four distinct supercritical flow regimes, depending on the location of the normal shock in relation with the behavior of the normalized activation function B of Paper I. Figure 1(a) shows the case of a supercritical flow, designated as regime I, in which the onset zone OZ is embedded in FGZ, where $dB/dx = O(1)$ numerically. In this case, the normal shock location ($z < x_l$) proceeds OZ and the nucleation rate decreases considerably by the jump at the shock location. Downstream of the normal shock a relatively thin subsonic nucleation zone followed by a droplet growth zone, where the flow is accelerated back to supersonic speeds, takes place. In Fig. 1(b) we distinguish the case of a supercritical flow, designated as regime II, in which the onset zone OZ, as in subcritical flows, is embedded in RGZ, where $dB/dx = O(K^{1/2})$, but ends at the shock front z prior to the relative onset point $x_l (z < x_l)$. Downstream is the local subsonic zone NZ followed by an ultimate supersonic flow in DGZ. Figure 1(c) presents the case of a supercritical flow, designated as regime III, where the normal shock proceeds the relative onset point ($z > x_l$). In this case the normal shock is embedded in NZ, which is followed by DGZ, where the flow is accelerated back to supersonic speeds. Finally, Fig. 1(d) shows the case of a supercritical flow, designated as regime IV, where the normal shock is embedded in the droplet growth zone ($z > x_l$). Once again, the

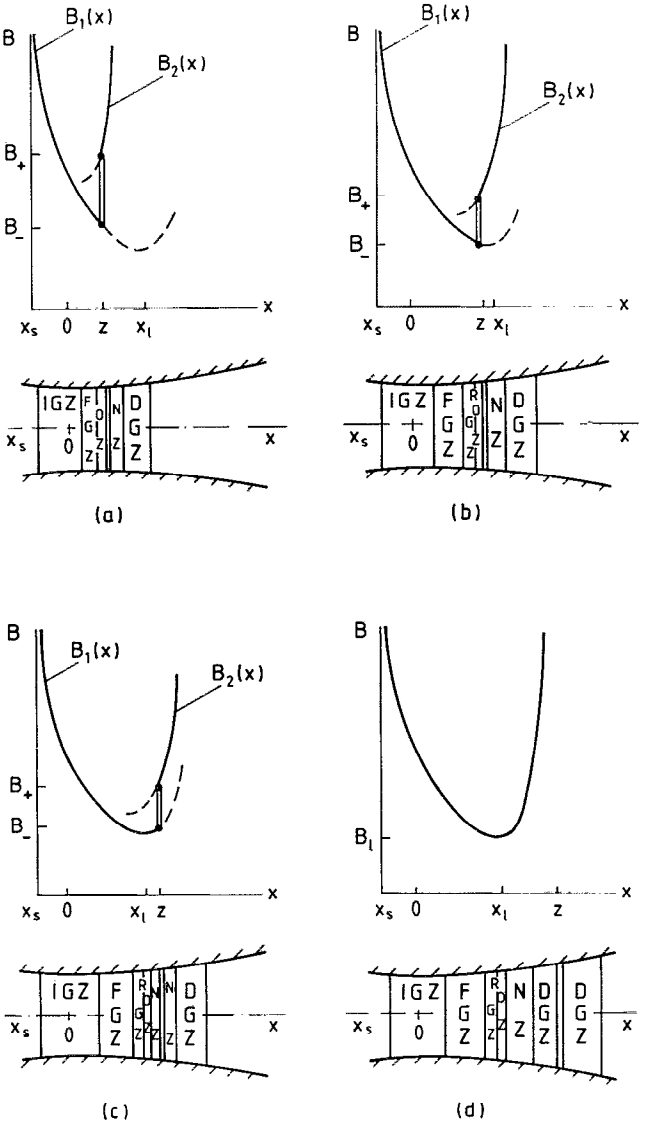

FIG. 1. Classification scheme for supercritical flows. (a) Regime I; (b) regime II; (c) regime III; and (d) regime IV. (Here x_s is the saturation point, $x=0$ is the throat location, z is the normal shock location, and x_l is the turning point of the activation function B.)

usual structure of a local subsonic zone followed by a supersonic zone occurs downstream of the shock. In a thermally choked flow any of the above supercritical regimes may occur, the particular choice depending on the location z of the normal shock fixed by a nucleation rate, sufficient for realizing the onset of condensation and by the nozzle geometry downstream of this onset zone.

B. Asymptotic solution of the rate equation in supercritical flow regimes

In supercritical flows the asymptotic analysis of the rate equation of Paper I applies only in the condensation zones upstream of the normal shock, i.e., for $x<z$. Thus, for a complete description of supercritical flows it is essential to carry out similar analysis downstream of the normal shock. This requires asymptotic analysis of Eq. (6) in different supercritical flow regimes.

In regime I the asymptotic analysis of the rate equation in IGZ and FGZ of Paper I remains valid upstream of the normal shock [Fig. 1(a)]. The novel feature upstream of the normal shock location is that the onset zone OZ is now embedded in FGZ, thereby its analytical structure is similar to that of FGZ of Paper I. Consequently, it suffices to carry out the asymptotic analysis of the rate equation (6) in the zones NZ and DGZ of Fig. 1(a) in the double limit as $K\to 0$ and $\lambda\to\infty$. This is done in Appendix A of this paper, where the asymptotic expressions for g in the zones NZ and DGZ downstream of the normal shock are explicitly exhibited. Regime II is realized when the location of the normal shock falls in RGZ of Paper I [Fig. 1(b)]. In such a case the nucleation rate decreases considerably by a jump at the shock location before possibly reaching the maximum accessible value if the flow were to be continued downstream continuously ($z\lesssim x_l$). In this case the structure of the onset zone and the flow upstream of the shock location are the same as in subcritical flow. Downstream of the normal shock the asymptotic expressions for g in the zones NZ and DGZ of Fig. 1(b) of this regime are given in Appendix B. In regime III the location of the normal shock falls in NZ ($z\gtrsim x_l$), as shown in Fig. 1(c). In this regime the solution for subcritical flow of Paper I remains unaltered up to the shock location in NZ. Similar to the analysis of regimes I and II of Appendices A and B, the asymptotic solution of the rate equation (6) in the zones NZ and DGZ of this regime downstream of the normal shock is presented in Appendix C. In regime IV the normal shock wave is embedded in the droplet growth zone DGZ [Fig. 1(d)]. Consequently, the asymptotic analysis in distinct condensation zones of Paper I remains unaltered up to the shock location, i.e., for $x<z$, where z now lies in DGZ. Naturally the droplet growth zone splits into two regions (upstream and downstream regions relative to the shock location). In the upstream region of DGZ the scaling variables and asymptotic expression for g are precisely those given in DGZ of Paper I. The asymptotic expression for g in the zone DGZ downstream of the normal shock can be found in Appendix D.

Combining the above summarized asymptotic solutions for g in the condensation zones downstream of the normal shock in each regime with those of Paper I upstream of the normal shock, together with the functional relations (8)–(12) of Paper I and the normal shock relations, we obtain the local asymptotic solution for supercritical flows in the corresponding regime, provided that we know the normal shock location z. In this case for the sign in front of the square root in Eq. (8) of Paper I, the (+) sign should be chosen in the supersonic region upstream of the normal shock, the (−) sign in the local subsonic region downstream of the normal shock, and the (+) sign again far downstream of the normal shock when the accelerated flow reaches supersonic speeds once again. In order to develop an algorithm for asymptotic predictions of supercritical flows in each regime, we need to supplement the above asymptotic analysis by the normal shock relations and discuss how we can determine the normal shock location z.

V. NORMAL SHOCK RELATIONS AND SHOCK STRENGTH IN CONDENSING NOZZLE FLOWS

The normal shock relations of the flow variables for condensing flows are well known.[14] In thermally choked flows the functional $\Delta(g,x)$ of Eq. (1) plays the most important role; therefore, it is essential to exhibit the normal shock relations for condensing flows in relation to the functional $\Delta(g,x)$. It follows directly from Eqs. (1)–(4), together with the continuity of g at $x=z$ that

$$\Delta_{\pm}=\left(\frac{1+u_s^2+R_z}{2u_s}\right)^2-\Theta_z\left(T_0+\frac{L(T_{\pm})}{c_{p0}}g_z\right), \tag{9}$$

where we have used the subscript z to denote the value of any continuous function or functional at the shock location [e.g., $g_z\equiv g(z)$, $\Theta_z\equiv\Theta(g_z)$, $R_z\equiv R(g,z)$, etc.]. It follows immediately from Eq. (9) that the normal shock relation for Δ is of the form

$$\delta\Delta\equiv\Delta_+-\Delta_-=-\frac{\Theta_z g_z}{c_{p0}}\delta L, \tag{10}$$

where $\delta L\equiv L(T_+)-L(T_-)$. This shows that the functional $\Delta(g,x)$ is discontinuous at $x=z$ unless the latent heat L is a constant. Since $T_+>T_-$ and L is a decreasing function of T for most fluids, it follows that for most fluids $\delta\Delta>0$, i.e., $\Delta(g,x)$ shows an increase across the normal shock due to temperature dependence of the latent heat. The flow speeds u_+ just upstream and u_- just downstream of the normal shock now follow from the functional relation for $u(g,x)$ of Paper I as

$$u_{\pm}=\frac{(1+u_s^2+R_z)/(2u_s)\mp\sqrt{\Delta_{\pm}}}{[1+\gamma+(\gamma-1)H^{-1}g_z]/(2\gamma)}; \tag{11}$$

Eq. (11) immediately leads to the normal shock relation for u, namely,

$$\delta u\equiv u_+-u_-=-\frac{2\gamma(\sqrt{\Delta_+}+\sqrt{\Delta_-})}{1+\gamma+(\gamma-1)H^{-1}g_z}<0. \tag{12}$$

The normal shock relations for the rest of the variables follow from the corresponding functional relations as

$$\delta\rho \equiv \rho_+ - \rho_- = -\frac{u_s}{A_z (u^g)^2}\,\delta u > 0, \tag{13}$$

$$\delta p \equiv p_+ - p_- = -\frac{u_s}{A_z}\,\delta u > 0, \tag{14}$$

$$\delta T \equiv T_+ - T_- = \frac{g_z}{c_{p0}}\,\delta L - \frac{u^a}{c_{p0}}\,\delta u > 0, \tag{15}$$

where u^a and u^g, respectively, denote the arithmetic mean and the geometric mean of u_+ and u_-, i.e.,

$$u^a \equiv \frac{u_+ + u_-}{2} \tag{16}$$

and

$$u^g \equiv \sqrt{u_+ u_-}. \tag{17}$$

It is straightforward to show that the above normal shock relations are equivalent to the classical ones. The normal shock relations (12)–(15), together with Eqs. (9), (11), (16), and (17), solve for the variables with subscript (+) just upstream of the normal shock in terms of those with subscript (−) just downstream of the normal shock. This solution is implicit since $L(T_+)$ is not known *a priori*. The procedure to obtain the solution is to first assume an initial guess for $L(T_+)$ [this initial guess may as well be set equal to $L(T_-)$] and then to correct for it iteratively using the normal shock relations, until a reasonable agreement between the resulting computed value and the initial guess is achieved. In cases where L is treated as a constant ($\delta L \equiv 0$), the above implicit solution turns into an explicit one, since by Eq. (10) $\delta\Delta \equiv 0$, thereby the functional $\Delta(g,x)$ becomes continuous at $x=z$ at the value $\Delta_z \equiv \Delta(g,z)$. In such a case δu of Eq. (12) and δT of Eq. (15) simplify as

$$\delta u = -\frac{4\gamma\sqrt{\Delta_z}}{1+\gamma+(\gamma-1)H^{-1}g_z}, \tag{18}$$

$$\delta T = -\frac{u^a}{c_{p0}}\,\delta u, \tag{19}$$

and u^a and u^g of Eqs. (16) and (17) can be explicitly evaluated from

$$u^a = \frac{\gamma(1+u_s^2+R_z)}{u_s[1+\gamma+(\gamma-1)H^{-1}g_z]} \tag{20}$$

and

$$u^g = (1-H^{-1}g)\sqrt{\frac{T_0+(g_z L/c_{p0})}{\Theta_z}}. \tag{21}$$

Having exhibited the essential normal shock relations in condensing nozzle flows, it may be useful to discuss the strength of such shock waves. For this reason we denote the strength of the normal shock by Γ, as conventionally defined by

$$\Gamma \equiv \frac{\delta\rho}{\rho_-} = -\frac{\delta u}{u_+} > 0, \tag{22}$$

which by Eqs. (11) and (12) evaluates to

$$\Gamma = \frac{\sqrt{\Delta_-}+\sqrt{\Delta_+}}{(1+u_s^2+R_z)/(2u_s)-\sqrt{\Delta_+}}. \tag{23}$$

Introducing the bounded functional,

$$D(g,x) \equiv \frac{1+q(g,x)/c_{p0}T_0}{1+q^*(g,x)/c_{p0}T_0} = \frac{4u_s^2\Theta(g)[c_{p0}T_0+gL(T)]}{c_{p0}[1+u_s^2+R(g,x)]^2} \tag{24}$$

[obviously $0 < D(g,x) \leqslant 1$, for all $x>0$; and $D(g,x)$ is not, in general, continuous at $x=z$ unless L is a constant], which characterizes a measure of the amount of heat needed at any location x to thermally choke the flow, we can conveniently write Eq. (23) for the shock strength in the form

$$\Gamma = \frac{\sqrt{1-D_-}+\sqrt{1-D_+}}{1-\sqrt{1-D_+}}. \tag{25}$$

In the case of constant latent heat L where the functional $D(g,x)$ becomes continuous at $x=z$ so that $D_\pm = D_z \equiv D(g,z)$, Eq. (25) simplifies as

$$\Gamma = \frac{2\sqrt{1-D_z}}{1-\sqrt{1-D_z}}. \tag{26}$$

It follows immediately from Eq. (26) that for the case of constant latent heat Γ is a decreasing function of D_z. In particular, as $D_z \to 0$ (possible only if $T_0 \to 0$), we obtain $\Gamma \to \infty$. In general, an upper bound for Γ can, in principle, be found if a lower bound for the reservoir temperature $T_0 > 0$ is assumed. On the other hand, if isentropic flow conditions are taken for granted at the throat ($x=0$), then $D \to 1$; consequently $\Gamma \to 0$ as $z \to 0^+$, as expected.

VI. SHOCK FITTING

For a complete description of the asymptotic theory of supercritical nozzle flows, it remains to discuss how one can determine the shock location z (shock fitting). In this connection the functional $\Delta(g,x)$ given by Eq. (1) becomes the most important quantity. Thus a detailed analysis of $\Delta(g,x)$ and its total derivative $d\Delta/dx$ is now essential.

We first define the amount of heat $Q(g,x)$ needed at any location x to thermally choke the flow by

$$\frac{Q(g,x)}{c_{p0}T_0} \equiv \frac{q^*(g,x)}{c_{p0}T_0} - \frac{q(g,x)}{c_{p0}T_0}. \tag{27}$$

Now Eq. (1) becomes

$$\Delta(g,x) = T_0\Theta(g)\left(\frac{Q(g,x)}{c_{p0}T_0}\right), \tag{28}$$

which, by differentiation, leads to

$$\frac{d\Delta}{dx} = \frac{1}{\Theta(g)}\frac{d\Theta}{dg}\,\Delta(g,x)\,\frac{dg}{dx} + T_0\Theta(g)\,\frac{d}{dx}\left(\frac{Q(g,x)}{c_{p0}T_0}\right). \tag{29}$$

It is exhibited in Delale *et al.*[12] from the singularities of the differential equations characterizing nozzle flows with non-equilibrium condensation that necessary (but not sufficient) conditions for thermal choking are satisfied whenever

$$\Delta=0 \quad \text{and} \quad \frac{d}{dx}\left(\frac{Q(g,x)}{c_{p0}T_0}\right)=0, \tag{30}$$

or, equivalently, by Eq. (29),

$$\Delta=0 \quad \text{and} \quad \frac{d\Delta}{dx}=0, \tag{31}$$

at the singularities of the differential system. For subcritical flows these conditions are only realized at the throat ($x=0$) without heat addition, where the singularity is a saddle point. In the same paper it is also demonstrated that satisfying the conditions,

$$\Delta=0 \quad \text{and} \quad \frac{d}{dx}\left(\frac{Q(g,x)}{c_{p0}T_0}\right)<0, \tag{32}$$

at some point along the nozzle is sufficient for a flow to be thermally choked. Therefore, for a thermally choked flow the conditions given by Eq. (32) are satisfied at some point, which we, from now on, denote by $\hat{x}>0$ [Figs. 2(a) and 2(b)]. Since Δ is differentiable in the interval $(0,\hat{x})$ prior to thermal choking and $\Delta=0$ at $x=0$ and $x=\hat{x}$, it follows from Rolle's Theorem that there exists a point $x_m\in(0,\hat{x})$, where $d\Delta/dx=0$. It also follows from the continuity of the derivative $d/dx[Q(g,x)/(c_{p0}T_0)]$ in the interval $(0,\hat{x})$ that

$$\frac{d}{dx}\left(\frac{Q(g,x)}{c_{p0}T_0}\right)=0, \tag{33}$$

for some point $\bar{x}\in(0,\hat{x})$. Equation (30) now implies that $d\Delta/dx<0$ at $x=\bar{x}$ since $d\Theta/dg<0$. This proves the result

$$0<x_m<\bar{x}<\hat{x} \tag{34}$$

[also see Figs. 2(a) and 2(b)]. Since Δ necessarily becomes negative for $x>\hat{x}$, the flow must stop at $x=\hat{x}$, and the inclusion of a normal shock prior to this location becomes necessary. In principle, the normal shock location z may fall anywhere in the interval $(0,\hat{x})$. It is important to note that as $z\to\hat{x}^-$ or $z\to 0^+$, we obtain $D_z\to 1$, thus $\Gamma\to 0$. This shows that the shock weakens as the shock location z approaches either the throat ($x=0$) or the point $x=\hat{x}$. From this we can expect shocks of large or moderate strength to be found for $0<z<\bar{x}$. Weak shocks may be located in the interval $(\bar{x},\hat{x})$ or near the throat.

We are now in a position to introduce a relatively simple shock fitting technique. This technique is based on accelerating the flow downstream of the normal shock to supersonic speeds by passing through a saddle point located at $x=x^*$, where both Δ and $d\Delta/dx$ vanish. It is remarkable that the existence of a solution with the above property should be regarded as a necessary condition for the existence of stationary normal shock waves in thermally choked flows (to guarantee sufficiency, the formidable problem of stability of such shock waves should also be considered); otherwise the flow is unsteady, a case that will not be discussed in this paper. We first let z_1 and z_2 ($z_1<z_2$) be two points in the interval $(0,\hat{x})$ with the following property: If the location of the shock is chosen at z_1, then the downstream solution cannot accelerate to supersonic speeds, i.e., Δ remains positive for all $x>z_1$ [curve 1 in Fig. 2(a) or 2(b), depending on whether the latent heat is constant or not], and if the shock location is taken at z_2, then the downstream solution in the Δ-x plane crosses the $\Delta=0$ axis with a negative slope ($d\Delta/dx<0$), where the flow cannot continue [curve 2 in Fig. 2(a) or 2(b), depending on whether the latent heat is constant or not]. If we now choose any point, say z_3, in (z_1,z_2) as the shock location, the downstream solution then resembles either curve 1 of Fig. 2(a) or 2(b), depending on the latent

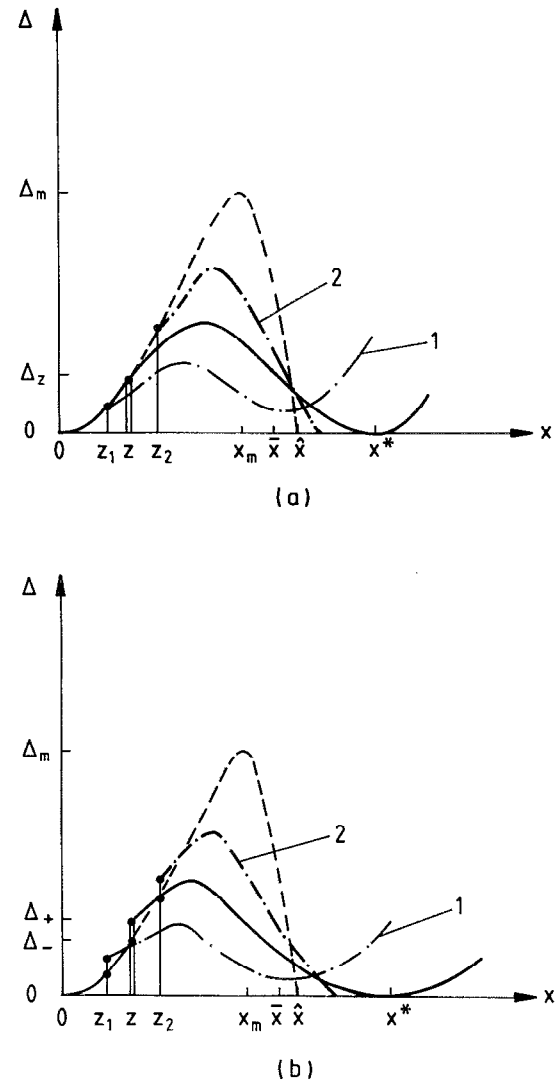

FIG. 2. Variation of the functional Δ along the nozzle in supercritical flows for (a) constant latent heat, (b) temperature dependent latent heat. ---, shock-free thermally choked flow; ——, supercritical flow solution with a stationary normal shock at z passing through a saddle point x^*, —·—, (curve 1) supercritical flow solution with shock location at $z_1<z$, where the flow cannot accelerate to supersonic speeds; –·–, (curve 2) supercritical flow solution with shock location at $z_2>z$, where the flow downstream cannot continue.

heat, for which $z\in(z_3,z_2)$ or curve 2 of Fig. 2(a) or 2(b), depending on the latent heat, for which $z\in(z_1,z_3)$. (The almost improbable case where z_3 is chosen by coincidence so that the downstream solution passes precisely through the saddle point x^* yields the right choice for the shock location, i.e., $z_3=z$.) The above procedure is repeated sequentially until the uncertainty in locating z, thus in achieving passage through the saddle point x^*, is within the desired degree of accuracy. When this occurs, it is important that the $(-)$ sign in front of $\sqrt{\Delta}$ in the subsonic branch of the functional $u(g,x)$ of Paper I [Eq. (8) in Paper I] should be changed to the $(+)$ sign whenever $x>x^*$. Finally, we should also mention that this simple and practical shock fitting technique is equivalent to the more complicated one employed by Barschdorff[5] and Clarke and Delale.[7]

VII. SUPERCRITICAL PREDICTIONS OF ASYMPTOTIC THEORY

We are now in a position to present an algorithm for computing supercritical nozzle flows. This algorithm naturally starts with the algorithm of Paper I for subcritical flows and follows the same procedure until the flow is thermally choked. This occurs when the functional $\Delta(g,x)$ vanishes at some point $x=\hat{x}$ downstream of the onset of condensation [Figs. 2(a) and 2(b)]. Now the flow is supercritical and if it is stationary, it falls in one of the four regimes presented in Sec. IV. Unfortunately, since the shock location z is not known *a priori*, it is difficult to determine which supercritical flow regime is achieved for fixed reservoir conditions, nozzle geometry, and working fluid in steady flows (it is important to mention that for fixed conditions of a thermally choked flow, we assume that only one of the four regimes can be realized in steady flows). Therefore, in the algorithm we include all the four regimes, the appropriate choice depending on the shock location z.

In regime I the algorithm of Paper I for computing subcritical flows remains valid upstream of the shock location, which we choose to be within a finite distance upstream of the point $x=x_l$ [Fig. 1(a)]. From the normal shock relations of Sec. V, we evaluate the flow conditions just behind the normal shock. Now the asymptotic expressions of regime I in Appendix A for NZ and DGZ downstream of the shock yield a downstream solution. From the shock fitting technique of Sec. VI it is obvious that this downstream solution corresponds to a situation of the form of either curve 1 or curve 2 of Figs. 2(a) and 2(b). If the downstream solution is of the form of curve 1 of Figs. 2(a)–2(b), i.e., if the flow is not accelerated back to supersonic speeds, the assumed shock location should be moved toward the point x_l. In case the downstream solution is of the form of curve 2 of Figs. 2(a) and 2(b), the assumed shock location should be moved toward the throat $x=0$. This procedure is repeated until the shock is located in this regime within a desired degree of accuracy. If this is not possible, we proceed to regimes II or III [Figs. 1(b) and 1(c)]. In these regimes the same procedure applies, now utilizing the asymptotic expressions of Appendices B and C, except that the initial guess for the shock location is now within a distance of $O(K^{1/2})$ upstream of x_l in regime II and downstream of x_l in regime III. If no location of shock with the desired downstream solution is achieved in these regimes either, we proceed to regime IV. In this regime the downstream solution is achieved similarly, utilizing the asymptotic expressions of Appendix D together with the shock fitting technique of Sec. VI, so that the shock location lies in DGZ [Fig. 1(d)]. For a thermally choked flow if the shock cannot be located in any of the four supercritical flow regimes, we conclude that the flow is unsteady (this case is excluded from discussion in this paper).

The above algorithm is used for the supercritical predictions of moist air expansions under atmospheric supply conditions using three different nozzles. In addition to the circular arc nozzles (nozzles 1 and 2) of Paper I, the hyperbolic arc nozzle (nozzle 3) with throat height $2y^*=120$ mm and with radius of curvature of the throat arc $R^*=200$ mm is employed to demonstrate an interesting critical case of a flow bordering on supercritical flows. Nozzle 1, as already mentioned in Paper I, is one dimensional, whereas nozzles 2 and 3 are effectively two dimensional. The classical nucleation rate equation and the Hertz–Knudsen droplet growth law are employed so that the thermodynamic functions and parameters entering the asymptotic theory are precisely those given in Paper I. The properties of the condensed phase are taken from those of the liquid and ice models of Paper I. The initial relative humidity is in the range of 40%–80% under atmospheric supply conditions, and the onset point is defined as the point where the condensate mass fraction assumes the value $g_k' = 0.1$ g/kg (notice the change in definition from that for subcritical moist air expansions of Paper I). As in Paper I, all the primed variables herein denote actual values.

Figures 3–5 show the predictions of the asymptotic theory for supercritical expansion of moist air with atmospheric supply conditions through nozzle 1, as compared to the two-dimensional (2-D) finite volume computations by Schnerr and Dohrmann,[15] and the recent experimental data by Schnerr.[13] As in subcritical flows, the predictions of the 1-D and 2-D adiabatic pressure distributions along the axis of this nozzle seem to agree well. Just as in subcritical flows, for this nozzle the predictions of the 1-D asymptotic theory for the diabatic pressure distribution downstream of the condensation zones yield values that are a few percent higher than the experimentally measured ones. In particular, Fig. 3(a) shows the Mach number contours in nozzle 1, which demonstrates that the flow through this nozzle is nearly one dimensional, at least in the condensation zones of interest. In Fig. 3(b) the predictions of the 1-D asymptotic theory is presented in comparison with the 2-D finite volume computations of Schnerr and Dohrmann[15] in the ice model with $\alpha=0.2$, where no good agreement of the asymptotic predictions with experimental data[13] is achieved (the predicted shock location is a few millimeters downstream of the location visualized by schlieren photographs). Figure 4 shows the

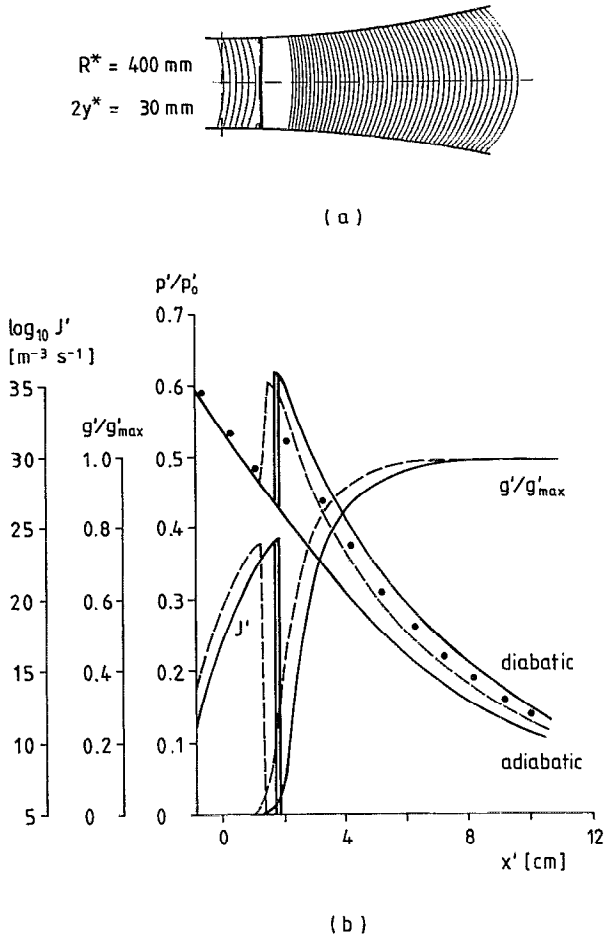

FIG. 3. (a) The Mach number contours from the numerical 2-D simulation of Schnerr and Dohrmann[15] in nozzle 1 under the atmospheric supply conditions $\varphi_0=73.4\%$, $\omega_0=7.3$ g/kg, $T_0'=287.2$ K (the increment between any two successive contours is $\Delta M=0.02$). (b) Distribution of the pressure, the nucleation rate, and the condensate mass fraction along the axis of nozzle 1 under the atmospheric supply conditions $\varphi_0=73.4\%$, $\omega_0=7.3$ g/kg, $T_0'=287.2$ K. ●, static pressure measurements in experiments conducted by Schnerr[13] (observed shock location $z_{ob}'=12$ mm). ----, numerical 2-D finite volume computations in the ice model with $\alpha=0.2$ by Schnerr and Dohrmann[15] ($T_s'=281.5$ K, $T_k'=230.8$ K, $\Delta T_{ad}'\equiv T_s'-T_k'=50.7$ K, $M_k=1.105$, $J_{max}'=0.86\times10^{24}$ m^{-3} sec^{-1}). ——, supercritical 1-D asymptotic solution in the ice model with $\alpha=0.2$ ($T_s'=281.5$ K, $T_k'=224.1$ K, $\Delta T_{ad}'=T_s'-T_k'=57.4$ K, $M_k=1.19$, $J_{max}'=0.103\times10^{25}$ m^{-3} sec^{-1}, $z'=18$ mm, $\Gamma=0.317$, $K=0.119\times10^{-1}$, and $\lambda=548.4$).

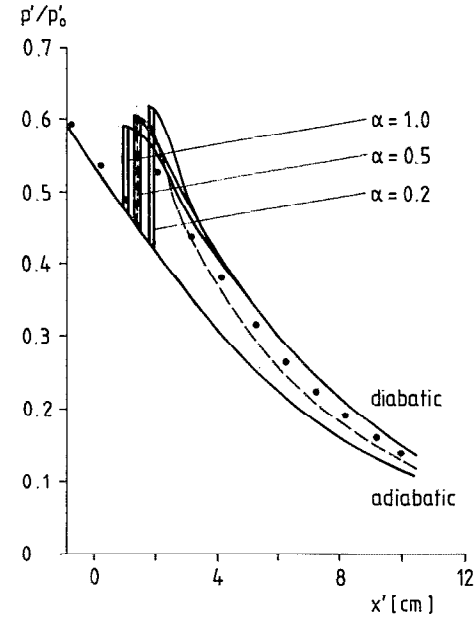

FIG. 4. The pressure distribution along the axis of nozzle 1 in the ice model with different values of the condensation coefficient α under the atmospheric supply conditions of Fig. 3. ●, experimental measurements by Schnerr[13] (observed shock location $z_{ob}'=12$ mm). ---, numerical 2-D finite volume computations with $\alpha=0.2$ by Schnerr and Dohrmann.[15] ——, supercritical 1-D asymptotic solution (for $\alpha=0.2$, $z'=18$ mm; for $\alpha=0.5$, $z'=12$ mm; for $\alpha=1.0$, $z'=9$ mm).

pressure distributions and shock locations of the 1-D asymptotic theory for the same reservoir conditions in nozzle 1 for different values of α in the ice model. As in subcritical flows better agreement with the static pressure distribution and in this case with the observed shock location is achieved if α is taken between 0.5 and 0.6, in contrast to the value 0.2 of 2-D numerical computations of Schnerr and Dohrmann.[15] On the other hand, the predictions of the 1-D asymptotic theory for the same initial flow conditions in nozzle 1, employing the liquid model, seem to agree even better with the pressure measurements, observed shock location, and shock strength (deduced from pressure measurements), as shown in Fig. 5. Therefore we conclude that for the supercritical expansion of moist air with atmo-

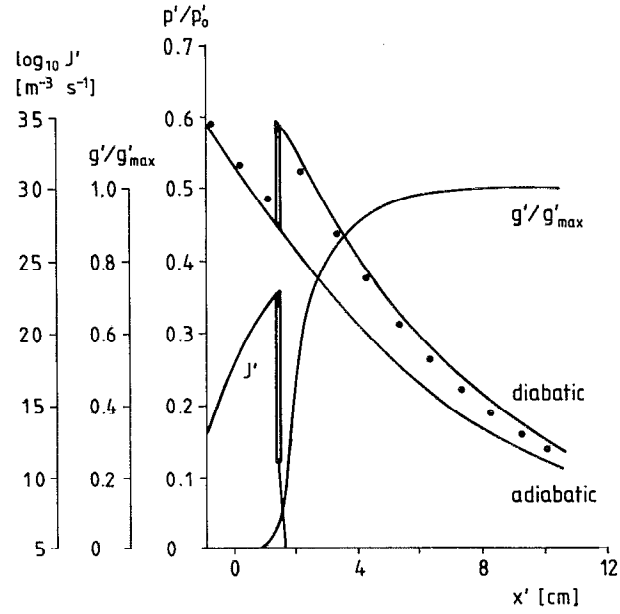

FIG. 5. Distribution of the pressure, the nucleation rate, and the condensate mass fraction along the axis of nozzle 1 under the atmospheric supply conditions $\varphi_0=73.4\%$, $\omega_0=7.3$ g/kg, and $T_0'=287.2$ K. ●, static pressure measurements in experiments conducted by Schnerr[13] (observed shock location $z_{ob}'=12$ mm). ——, supercritical 1-D asymptotic solution in the liquid model where $\alpha=1.0$ for $x\gg x_k$ ($T_s'=281.5$ K, $T_k'=227.2$ K, $\Delta T_{ad}'\equiv T_s'-T_k'=54.3$ K, $M_k=1.123$, $J_{max}'=0.23\times10^{23}$ m^{-3} sec^{-1}, $z'=12$ mm, $\Gamma=0.205$, $K=0.119\times10^{-1}$, and $\lambda=6938.3$).

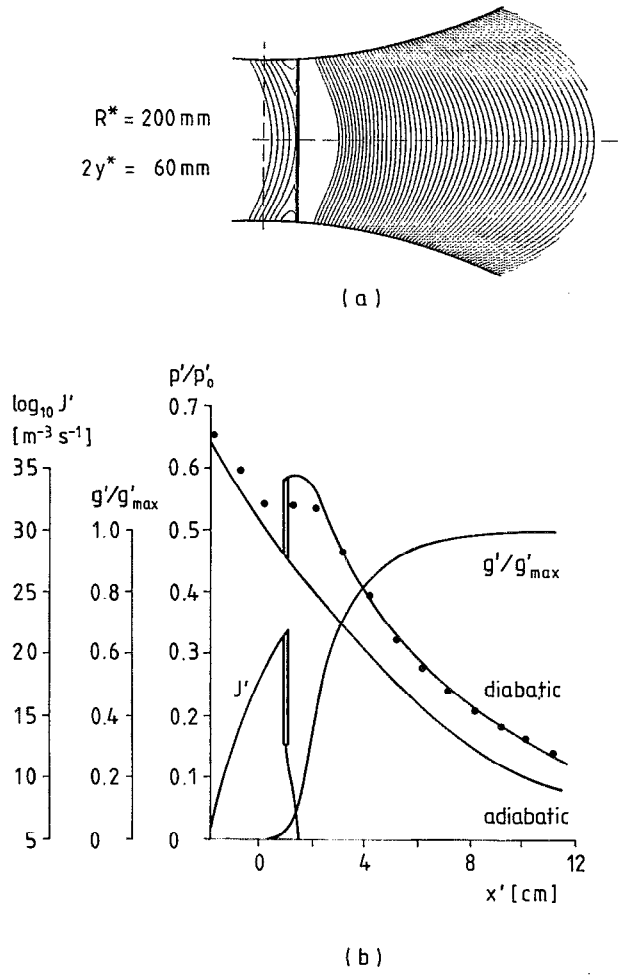

FIG. 6. (a) The Mach number contours from the numerical 2-D simulation of Schnerr and Dohrmann[15] in nozzle 2 under the atmospheric supply conditions $\varphi_0=75.3\%$, $\omega_0=8.15$ g/kg, and $T_0'=288.1$ K (the increment between any two successive contours is $\Delta M=0.02$). (b) Distribution of the pressure, the nucleation rate, and the condensate mass fraction along the axis of nozzle 2 under the atmospheric supply conditions $\varphi_0=75.3\%$, $\omega_0=8.15$ g/kg, and $T_0'=288.1$ K. ●, static pressure measurements in experiments conducted by Schnerr[13] (observed shock location $z_{ob}'=12$ mm). ——, supercritical 1-D asymptotic solution in the liquid model, where $\alpha=1.0$ for $x\geqslant x_k$ ($T_s'=282.9$ K, $T_k'=228.9$ K, $\Delta T_{ad}'\equiv T_s'-T_k'=54$ K, $M_k=1.103$, $J'_{max}=0.7\times10^{22}$ m^{-3} sec^{-1}, $z'=10$ mm, $\Gamma=0.169$, $K=0.116\times10^{-1}$, and $\lambda=19\,020.8$).

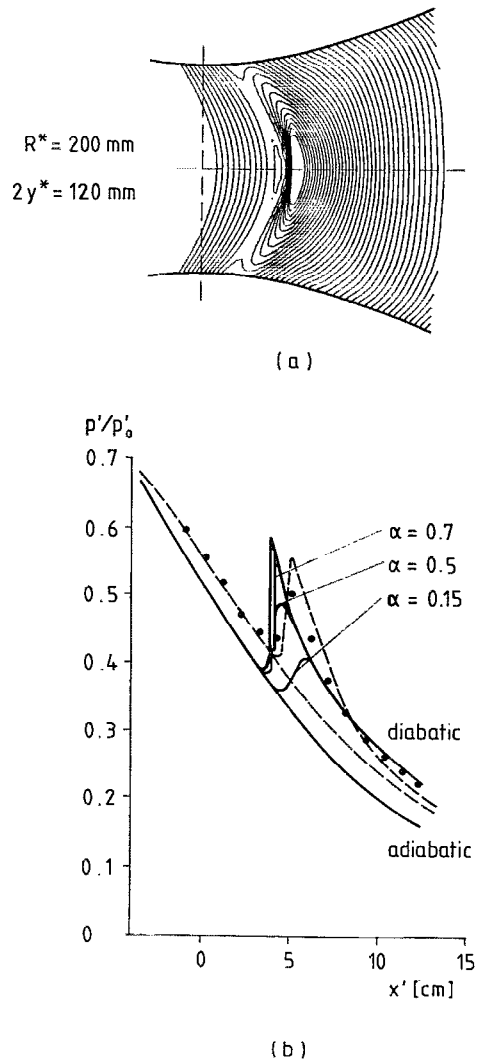

FIG. 7. (a) The Mach number contours from the numerical 2-D simulation of Schnerr and Dohrmann[15] in nozzle 3 under the atmospheric supply conditions $\varphi_0=42.1\%$, $\omega_0=8.78$ g/kg, and $T_0'=298.7$ K (the increment between any two successive contours is $\Delta M=0.02$). (b) The pressure distribution along the axis of nozzle 3 in the ice model with different values of the condensation coefficients α under the atmospheric supply conditions $\varphi_0=42.1\%$, $\omega_0=8.78$ g/kg, $T_0'=298.7$ K. ●, experimental measurements by Schnerr;[13] ---, numerical 2-D finite volume computations with $\alpha=0.15$ by Schnerr and Dohrmann[15] ($T_s'=282.2$ K, $T_k'=232.7$ K, $\Delta T_{ad}'\equiv T_s'-T_k'=49.5$ K, $M_k=1.191$, $J'_{max}=0.58\times10^{24}$ m^{-3} sec^{-1}); ——, 1-D asymptotic solution (for $\alpha=0.15$ and 0.5 we have subcritical flow, whereas for $\alpha=0.7$ we have supercritical flow, with a normal shock located at $z'=40$ mm; $K=0.838\times10^{-2}$, $\lambda=3186.4$).

spheric supply conditions through relatively slender nozzles like nozzle 1, better agreement with the experimental data for the pressure distribution and shock location is achieved by the 1-D asymptotic theory if the condensed phase is assumed to consist purely of water drops, a conclusion reached for subcritical flows as well. Figure 6 exhibits the predictions of the 1-D asymptotic theory in the liquid model for the supercritical expansion of moist air through nozzle 2 [which is obviously two dimensional, as can be demonstrated from the Mach number contours of Fig. 6(a)] against the experimental data of Schnerr.[13] In this case the adiabatic pressure distribution differs considerably from that of one dimension, and the normal shock location is shifted upstream, which should be considered as a 2-D effect. As in subcritical flows through effectively 2-D nozzles, in contrast to the upstream pressure distribution the downstream diabatic pressure distribution agrees well with the experimental measurements. This shows that the 1-D asymptotic theory cannot yield a satisfactory description for the entire 2-D supercritical flow field, and therefore should be modified to account for 2-D effects arising from nozzle wall curvature.

In all the predictions presented in Figs. 3–6, the supercritical flow falls in regime I. It would be interesting to compute a case of a supercritical flow that falls in other regimes. Figure 7 shows the predictions of the 1-D asymp-

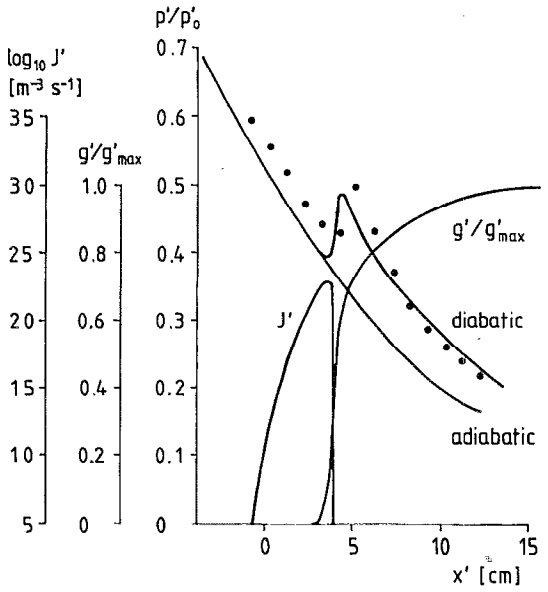

FIG. 8. Distribution of the pressure, the nucleation rate, and the condensate mass fraction along the axis of nozzle 3 with atmospheric supply conditions exhibited in Fig. 7. ●, static pressure measurements in experiments conducted by Schnerr.[13] ——, subcritical 1-D asymptotic solution in the liquid model, where $\alpha=1.0$ for $x>x_k$ ($T_s'=281.9$ K, $T_k'=228.4$ K, $\Delta T_{ad}'\equiv T_s'-T_k'=53.5$ K, $M_k=1.243$, $J_{max}'=0.82\times10^{23}$ m^{-3} sec^{-1}, $K=0.838\times10^{-2}$ and $\lambda=40\,249.7$).

totic theory for such a case through nozzle 3 (which is effectively 2D) in the ice model. In this case it can be demonstrated that whenever $\alpha>0.54$ (correct to two decimal places), the flow is supercritical, falling in regimes III or IV, depending on the value of α, whereas the flow remains subcritical for $\alpha<0.54$. On the other hand, the predictions of the 1-D asymptotic theory in the liquid model for this case, as shown in Fig. 8, demonstrate that the flow is really subcritical (naturally deviations from experimental measurements in this case occur due to 2-D effects). Flows resembling this example can be regarded as flows bordering on supercritical heat addition, and may as well be called "near critical flows."

VIII. CONCLUDING REMARKS

In this work a detailed analysis of supercritical nozzle flows with stationary normal shock waves is presented. A classification scheme based on the location of such normal shock waves, which distinguishes four distinct supercritical regimes is given, and the asymptotic solution of the condensation rate equation in each regime is worked out. A simple shock fitting technique is introduced to determine the shock location. An algorithm for the supercritical expansion of moist air under atmospheric supply conditions, which employs the classical nucleation theory and the Hertz–Knudsen droplet growth law, together with the liquid and ice models of the condensed phase of Paper I, is developed by exhibiting the asymptotic solution in each supercritical flow regime. Three distinct nozzles, 1, 2, and 3, nozzle 1 relatively slender, the others effectively two dimensional, are used. The following is demonstrated by the above developed algorithm.

(i) The supercritical asymptotic predictions of moist air expansions with atmospheric supply conditions through relatively slender nozzles like nozzle 1 yield good agreement with the measured static pressure distribution and the visualized shock location when the liquid model for the condensed phase is employed.

(ii) In supercritical moist air expansions with atmospheric supply conditions through 2-D nozzles like nozzles 2 and 3, even when the liquid model is employed, the shock seems to be located upstream of its visualized position and the 1-D pressure distribution differs considerably from the measured upstream distribution, in spite of the fact that somehow good agreement is achieved downstream of the shock.

(iii) In flows bordering on supercritical heat addition, called "near critical flows," either a subcritical flow pattern with very steep gradients or a supercritical flow pattern with a weak shock is observed in the liquid model, whereas in the ice model under the same reservoir conditions and nozzle geometry the flow may be supercritical or subcritical depending on the value assumed for the condensation coefficient α.

(iv) The majority of supercritical flows considered fall in regime I, whereas regimes III and IV seem to be realized in "near critical flows."

ACKNOWLEDGMENTS

The authors are grateful to Dr. U. Dohrmann for providing the 2-D finite volume computations shown in Figs. 3 and 7.

One of the authors (C.F.D.) acknowledges the support by the Alexander von Humboldt Foundation during the performance of this work.

APPENDIX A: ASYMPTOTIC SOLUTION OF THE RATE EQUATION DOWNSTREAM OF THE NORMAL SHOCK IN REGIME I

We herein assume that in Eq. (6) the thermodynamic functions $r_1^*(\xi)$, $\Sigma_1(\xi)$, $B_1(\xi)$, and $\Omega_1(\xi)$, all defined for $x_s\leqslant\xi\leqslant z$, are left-differentiable, whereas the thermodynamic functions $r_2^*(\xi)$, $\Sigma_2(\xi)$, $B_2(\xi)$, and $\Omega_2(\xi)$, all defined for $\xi\geqslant z$, are right-differentiable as many times as necessary at $\xi=z$ (note that all these functions are not even continuous at $\xi=z$). Using Laplace's method for an end point minimum as $\xi\to z^-$ in the first integral and as $\xi\to z^+$ in the second integral of Eq. (6), together with the double limit as $K\to0$ and $\lambda\to\infty$, we arrive at the asymptotic expression for the normalized condensate mass fraction g in the form

$$g(\psi)=b_-[(r_-^*+a_+\psi)^3+3a_-(r_-^*+a_+\psi)^2+6a_-^2(r_-^*+a_+\psi)+6a_-^3]+b_+[(r_+^*+a_+\psi)^3\times G_0(\psi)-3a_+(r_+^*+a_+\psi)^2G_1(\psi)+3a_+^2(r_+^*+a_+\psi)G_2(\psi)-a_+^3G_3(\psi)], \quad \text{(A1)}$$

where

$$\psi\equiv K^{-1}\left(\frac{dB}{dx}\right)_+(x-z)\geqslant 0, \quad \text{(A2)}$$

$$G_0(\psi)\equiv 1-e^{-\psi}, \quad \text{(A3)}$$

$$G_1(\psi)\equiv 1-(1+\psi)e^{-\psi}, \quad \text{(A4)}$$

$$G_2(\psi)\equiv 2-(2+2\psi+\psi^2)e^{-\psi}, \quad \text{(A5)}$$

$$G_3(\psi)\equiv 6-(6+6\psi+3\psi^2+\psi^3)e^{-\psi}, \quad \text{(A6)}$$

$$a_-\equiv -\lambda\Omega_-K\left(\frac{dB}{dx}\right)_-^{-1}>0, \quad \text{(A7)}$$

$$a_+\equiv \lambda\Omega_+K\left(\frac{dB}{dx}\right)_+^{-1}>0, \quad \text{(A8)}$$

$$b_-\equiv -\Sigma_-A_zK\left(\frac{dB}{dx}\right)_-^{-1}\exp(-K^{-1}B_-)>0, \quad \text{(A9)}$$

$$b_+\equiv \Sigma_+A_zK\left(\frac{dB}{dx}\right)_+^{-1}\exp(-K^{-1}B_+)>0, \quad \text{(A10)}$$

and where $(dB/dx)_\pm$ is to be evaluated from

$$\left(\frac{dB}{dx}\right)_\pm=\left(\frac{\partial\tilde{B}}{\partial g}\right)_\pm\left(\frac{dg}{dx}\right)_\pm+\left(\frac{\partial\tilde{B}}{\partial x}\right)_\pm. \quad \text{(A11)}$$

In particular, as $\psi\to\infty$, Eq. (9) becomes

$$g(\psi)\sim b_-[(r_-^*+a_+\psi)^3+3a_-(r_-^*+a_+\psi)^2+6a_-^2(r_-^*+a_+\psi)+6a_-^3]+b_+[(r_+^*+a_+\psi)^3-3a_+(r_+^*+a_+\psi)^2+6a_+^2(r_+^*+a_+\psi)-6a_+^3]. \quad \text{(A12)}$$

Obviously this cubic growth law that corresponds to a vanishing nucleation rate cannot persist throughout DGZ downstream of NZ. Taking into account the approach of the rate equation to saturated equilibrium states, the appropriate asymptotic expression for g in DGZ of regime I takes the form

$$g(x;K)=(b_-+b_+)\lambda^3\Omega_+^3[\hat{R}(x;K)]^3+3[b_-(r_-^*+a_-)+b_+(r_+^*-a_+)]\lambda^2\Omega_+^2[\hat{R}(x;K)]^2+3[b_-(r_-^{*2}+2a_-r_-^*+2a_-^2)+b_+(r_+^{*2}-2a_+r_+^*+2a_+^2)]\lambda\Omega_+\hat{R}(x;K)+[b_-(r_-^{*3}+3a_-r_-^{*2}+6a_-^2r_-^*+6a_-^3)+b_+(r_+^{*3}-3a_+r_+^{*2}+6a_+^2r_+^*-6a_+^3)], \quad \text{(A13)}$$

where

$$\hat{R}(x;K)\equiv\int_z^x\frac{\Omega_2(\xi;K)}{\Omega_+}d\xi. \quad \text{(A14)}$$

Introducing the scaling variables $\chi_{\rm I}$ and $R_{\rm I}$ by

$$\chi_{\rm I}\equiv\Lambda_{\rm I}K^{-2/3}(x-z), \quad \text{(A15)}$$

$$R_{\rm I}\equiv\Lambda_{\rm I}K^{-2/3}\hat{R}(x;K), \quad \text{(A16)}$$

with

$$\Lambda_{\rm I}\equiv[(b_-+b_+)K^2]^{1/3}\lambda\Omega_+, \quad \text{(A17)}$$

we obtain the asymptotic formula for g in DGZ of regime I as

$$g=R_{\rm I}^3+\epsilon_2^{\rm I}R_{\rm I}^2+\epsilon_1^{\rm I}R_{\rm I}+\epsilon_0^{\rm I}, \quad \text{(A18)}$$

where

$$\epsilon_0^{\rm I}\equiv[b_-(r_-^{*3}+3a_-r_-^{*2}+6a_-^2r_-^*+6a_-^3)+b_+(r_+^{*3}-3a_+r_+^{*2}+6a_+^2r_+^*-6a_+^3)], \quad \text{(A19)}$$

$$\epsilon_1^{\rm I}\equiv\frac{3[b_-(r_-^{*2}+2a_-r_-^*+2a_-^2)+b_+(r_+^{*2}-2a_+r_+^*+2a_+^2)]}{(b_-+b_+)^{1/3}}, \quad \text{(A20)}$$

$$\epsilon_2^{\rm I}\equiv\frac{3[b_-(r_-^*+a_-)+b_+(r_+^*-a_+)]}{(b_-+b_+)^{2/3}}, \quad \text{(A21)}$$

and where $R_{\rm I}$ satisfies the relaxation rate equation,

$$\frac{dR_{\rm I}}{d\chi_{\rm I}}=\hat{\Omega}, \quad \text{(A22)}$$

with $R_{\rm I}=0$ at $\chi_{\rm I}=0$ and $\hat{\Omega}\equiv\Omega_2/\Omega_+$. Herein, we should mention that the introduction of the scaling variables $\chi_{\rm I}$ and $R_{\rm I}$ given, respectively, by Eqs. (A15) and (A16) is based on the physical assumption that $(dB/dx)_+=O(1)$ on measure K and on the ordering of the double limit as $K\to 0$ and $\lambda\to\infty$, so that the physical condition $(dg/dx)_-=O(1)$ is fulfilled, namely

$$\lambda^3=O[K^{-3}\exp(K^{-1}B_-)], \quad \text{as } K\to 0. \quad \text{(A23)}$$

This ordering of the double limit is similar to that given in Blythe and Shih.[16]

APPENDIX B: ASYMPTOTIC SOLUTION OF THE RATE EQUATION DOWNSTREAM OF THE NORMAL SHOCK IN REGIME II

Similar to the procedure of Appendix A, the asymptotic solution of the rate equation (6) in NZ downstream of the shock in this regime can be written in the form

$$g(\psi)=d_-\left[(r_-^*+a_+\psi)^3 D_{-1}\left(\frac{\gamma_-}{\sqrt{2\beta_-}}\right)+3c_-(r_-^*+a_+\psi)^2 D_{-2}\left(\frac{\gamma_-}{\sqrt{2\beta_-}}\right)+6c_-^2(r_-^*+a_+\psi)D_{-3}\left(\frac{\gamma_-}{\sqrt{2\beta_-}}\right)\right.$$
$$\left.+6c_-^3 D_-\left(\frac{\gamma_-}{\sqrt{2\beta_-}}\right)\right]+b_+[(r_+^*+a_+\psi)^3 G_0(\psi)-3a_+(r_+^*+a_+\psi)^2 G_1(\psi)+3a_+^2(r_+^*+a_+\psi)G_2(\psi)-a_+^3 G_3(\psi)], \tag{B1}$$

where

$$\gamma_-\equiv -K^{-1}\left(\frac{dB}{dx}\right)_-\geqslant 0, \tag{B2}$$

$$\beta_-\equiv\frac{1}{2}K^{-1}\left(\frac{d^2B}{dx^2}\right)_->0, \tag{B3}$$

$$d_-\equiv\Sigma_- A_z(2\beta_-)^{-1/2}\exp\left(\frac{\gamma_-^2}{8\beta_-}\right)\exp(-K^{-1}B_-), \tag{B4}$$

$$c_-\equiv\lambda\Omega_-(2\beta_-)^{-1/2}, \tag{B5}$$

and where ψ, a_+, b_+, and $(dB/dx)_\pm$ are, respectively, given by Eqs. (A2), (A8), (A10), and (A11), the functions G_r, $r=0,1,2,3$ are given by Eqs. (A3)–(A6) of Appendix A, D_{-n}, $n=1,2,3,4$ are Whittaker's parabolic cylinder functions[17,18] and $(d^2B/dx^2)_-$ is evaluated from

$$\left(\frac{d^2B}{dx^2}\right)_-=\left(\frac{\partial\tilde{B}}{\partial g}\right)_-\left(\frac{d^2g}{dx^2}\right)_-+\left(\frac{\partial^2\tilde{B}}{\partial g^2}\right)_-\left(\frac{dg}{dx}\right)_-^2$$
$$+2\left(\frac{\partial^2\tilde{B}}{\partial g\,\partial x}\right)_-\left(\frac{dg}{dx}\right)_-+\left(\frac{\partial^2\tilde{B}}{\partial x^2}\right)_- \tag{B6}$$

In the limit as $\psi\to\infty$, the growth of g becomes cubic in ψ as

$$g(\psi)\sim d_-\left[(r_-^*+a_+\psi)^3 D_{-1}\left(\frac{\gamma_-}{\sqrt{2\beta_-}}\right)+3c_-(r_-^*+a_+\psi)^2 D_{-2}\left(\frac{\gamma_-}{\sqrt{2\beta_-}}\right)+6c_-^2(r_-^*+a_+\psi)D_{-3}\left(\frac{\gamma_-}{\sqrt{2\beta_-}}\right)\right.$$
$$\left.+6c_-^3 D_{-4}\left(\frac{\gamma_-}{\sqrt{2\beta_-}}\right)\right]+b_+[(r_+^*+a_+\psi)^3-3a_+(r_+^*+a_+\psi)^2+6a_+^2(r_+^*+a_+\psi)-6a_+^3], \tag{B7}$$

which cannot persist throughout DGZ . Following the procedure of regime I, the asymptotic solution of the rate equation for g in DGZ of regime II can be written in the form

$$g=R_{\rm II}^3+\epsilon_2^{\rm II}R_{\rm II}^2+\epsilon_1^{\rm II}R_{\rm II}+\epsilon_0^{\rm II}, \tag{B8}$$

where $R_{\rm II}$ and the scaling variable $\chi_{\rm II}$ are defined by

$$R_{\rm II}\equiv\Lambda_{\rm II}K^{-1/3}\hat{R}(x;K), \tag{B9}$$

$$\chi_{\rm II}\equiv\Lambda_{\rm II}K^{-1/3}(x-z)\geqslant 0, \tag{B10}$$

with

$$\Lambda_{\rm II}\equiv\left\{\left[d_-D_{-1}\left(\frac{\gamma_-}{\sqrt{2\beta_-}}\right)+b_+\right]K\right\}^{1/3}\lambda\Omega_+, \tag{B11}$$

satisfying the relaxation equation

$$\frac{dR_{\rm II}}{d\chi_{\rm II}}=\hat{\Omega}, \tag{B12}$$

subject to $R_{\rm II}=0$ at $\chi_{\rm II}=0$, and with $\hat{R}$ defined by Eq. (A14) of Appendix A, $\hat{\Omega}\equiv\Omega_2/\Omega_+$, and where

$$\epsilon_0^{\rm II}\equiv d_-\left[r_-^{*3}D_{-1}\left(\frac{\gamma_-}{\sqrt{2\beta_-}}\right)+3r_-^{*2}c_-D_{-2}\left(\frac{\gamma_-}{\sqrt{2\beta_-}}\right)\right.$$
$$\left.+6r_-^*c_-^2D_{-3}\left(\frac{\gamma_-}{\sqrt{2\beta_-}}\right)+6c_-^3D_{-4}\left(\frac{\gamma_-}{\sqrt{2\beta_-}}\right)\right]$$
$$+b_+(r_+^{*3}-3a_+r_+^{*2}+6a_+^2r_+^*-6a_+^3), \tag{B13}$$

$$\epsilon_1^{\rm II}\equiv 3\left\{d_-\left[r_-^{*2}D_{-1}\left(\frac{\gamma_-}{\sqrt{2\beta_-}}\right)+2c_-r_-^*D_{-2}\left(\frac{\gamma_-}{\sqrt{2\beta_-}}\right)\right.\right.$$
$$\left.+2c_-^2D_{-3}\left(\frac{\gamma_-}{\sqrt{2\beta_-}}\right)\right]+b_+(r_+^{*2}-2a_+r_+^*$$
$$\left.+2a_+^2)\right\}\left[d_-D_{-1}\left(\frac{\gamma_-}{\sqrt{2\beta_-}}\right)+b_+\right]^{-1/3}, \tag{B14}$$

$$\epsilon_2^{\rm II}\equiv 3\left\{d_-\left[r_-^*D_{-1}\left(\frac{\gamma_-}{\sqrt{2\beta_-}}\right)+c_-D_{-2}\left(\frac{\gamma_-}{\sqrt{2\beta_-}}\right)\right]\right.$$
$$\left.+b_+(r_+^*-a_+)\right\}\left[d_-D_{-1}\left(\frac{\gamma_-}{\sqrt{2\beta_-}}\right)+b_+\right]^{-2/3}. \tag{B15}$$

It is essential to mention that the appropriate scaling vari-

ables R_{II} and χ_{II} given, respectively, by Eqs. (B9) and (B10), are consistently obtained by assuming that $(dB/dx)_+ = O(1)$ on measure K, and by ordering the double limit as $K \to 0$ and $\lambda \to \infty$, such that $(dg/dx)_- = O(1)$, namely

$$\lambda^3 = O[K^{-3/2} \exp(K^{-1} B_-)], \quad \text{as } K \to 0. \tag{B16}$$

This ordering of the double limit is similar to that given in Clarke and Delale.[19]

APPENDIX C: ASYMPTOTIC SOLUTION OF THE RATE EQUATION DOWNSTREAM OF THE NORMAL SHOCK IN REGIME III

In this regime the asymptotic expression for g in NZ downstream of the normal shock follows from the asymptotic solution of the rate equation (6) as

$$g(\psi) = b_l\{(r_l^* + a_l\delta_l + a_+\psi)^3 F_0(\delta_l) - 3a_l(r_l^* + a_l\delta_l + a_+\psi)^2 F_1(\delta_l) + 3a_l^2(r_l^* + a_l\delta_l + a_+\psi)F_2(\delta_l) - a_l^3 F_3(\delta_l)\} + b_+[(r_+^* + a_+\psi)^3 G_0(\psi) - 3a_+(r_+^* + a_+\psi)^2 G_1(\psi) + 3a_+^2(r_+^* + a_+\psi)G_2(\psi) - a_+^3 G_3(\psi)], \tag{C1}$$

where, as in Paper I, a_l and b_l are given by

$$a_l \equiv \lambda \Omega \beta_l^{-1/2}, \tag{C2}$$

$$b_l \equiv \Sigma_l A_l \beta_l^{-1/2} \exp(-K^{-1} B_l), \tag{C3}$$

with

$$\beta_l \equiv \frac{1}{2} K^{-1} \left(\frac{d^2 B}{dx^2}\right)_l, \tag{C4}$$

the scaling coordinate ψ is defined by Eq. (A2) of Appendix A and δ_l is defined by

$$\delta_l \equiv \sqrt{\beta_l}(z - x_l) \geqslant 0, \tag{C5}$$

and where a_+ and b_+ are, respectively, given by Eqs. (A8) and (A10) and the functions G_r, $r=0,1,2,3$ are given by Eqs. (A3)–(A6) of Appendix A. The functions F_r, $r=0,1,2,3$, as in Paper I, are defined by

$$F_r(\phi) \equiv \int_{-\infty}^{\phi} \zeta^r e^{-\zeta^2} d\zeta; \quad r=0,1,2,3, \tag{C6}$$

and $(d^2B/dx^2)_l$ is evaluated from Eq. (B6) of Appendix B with the subscript $(-)$ replaced by the subscript l. As can easily be demonstrated when $\delta_l \to 0$ ($z^- \to x_l$ in regime II and $z^+ \to x_l$ in regime III), the structure of NZ and the asymptotic expressions in NZ (and consequently in all other zones) of regimes II and III coincide. Also worth mentioning is that as $\psi \to 0$ in the subsonic NZ of this regime, and as $\phi \to \delta_l$ in the supersonic NZ of subcritical flows, we recover the same expression for g, i.e., the continuity of g at $x=z$ is guaranteed.

In the limit as $\psi \to \infty$, Eq. (C1) becomes

$$g(\psi) \sim b_l\{(r_l^* + a_l\delta_l + a_+\psi)^3 F_0(\delta_l) - 3a_l(r_l^* + a_l\delta_l + a_+\psi)^2 F_1(\delta_l) + 3a_l^2(r_l^* + a_l\delta_l + a_+\psi)F_2(\delta_l) - a_l^3 F_3(\delta_l)\} + b_+[(r_+^* + a_+\psi)^3 - 3a_+(r_+^* + a_+\psi)^2 + 6a_+^2(r_+^* + a_+\psi) - 6a_+^3]. \tag{C7}$$

Similar to the procedure adopted in other regimes, this cubic growth of g will not persist downstream throughout DGZ, and in the approach to saturated thermodynamic equilibrium the condensate mass fraction in DGZ of this regime is governed by

$$g = R_{III}^3 + \epsilon_2^{III} R_{III}^2 + \epsilon_1^{III} R_{III} + \epsilon_0^{III}, \tag{C8}$$

where R_{III} and the scaling variable χ_{III} in DGZ of this regime are defined by

$$R_{III} \equiv \Lambda_{III} K^{-1/3} \hat{R}(x;K), \tag{C9}$$

$$\chi_{III} \equiv \Lambda_{III} K^{-1/3}(x - z) \geqslant 0, \tag{C10}$$

with $\hat{R}$ given by Eq. (A14) of Appendix A and

$$\Lambda_{III} \equiv \{[b_l F_0(\delta_l) + b_+]K\}^{1/3} \lambda \Omega_+, \tag{C11}$$

and where R_{III} is to be solved from the relaxation rate equation

$$\frac{dR_{III}}{d\chi_{III}} = \hat{\Omega}, \tag{C12}$$

subject to $R_{III} = 0$ at $\chi_{III} = 0$ with $\hat{\Omega} \equiv \Omega_2/\Omega_+$. The coefficients ϵ_0^{III}, ϵ_1^{III} and ϵ_2^{III} in Eq. (C8) are given as follows:

$$\epsilon_0^{III} \equiv b_l[(r_l^* + a_l\delta_l)^3 F_0(\delta_l) - 3a_l(r_l^* + a_l\delta_l)^2 F_1(\delta_l) + 3a_l^2(r_l^* + a_l\delta_l)F_2(\delta_l) - a_l^3 F_3(\delta_l)] + b_+(r_+^{*3} - 3a_+ r_+^{*2} + 6a_+^2 r_+^* - 6a_+^3), \tag{C13}$$

$$\epsilon_1^{III} \equiv 3\{b_l[(r_l^* + a_l\delta_l)^2 F_0(\delta_l) - 2a_l(r_l^* + a_l\delta_l)F_1(\delta_l) + a_l^2 F_2(\delta_l)] + b_+(r_+^{*2} - 2a_+ r_+^* + 2a_+^2)\} \times [b_l F_0(\delta_l) + b_+]^{-1/3}, \tag{C14}$$

$$\epsilon_2^{III} \equiv 3\{b_l[(r_l^* + a_l\delta_l)F_0(\delta_l) - a_l F_1(\delta_l)] + b_+(r_+^* - a_+)\}[b_l F_0(\delta_l) + b_+]^{-2/3}. \tag{C15}$$

It is essential to mention once again that the scaling variables R_{III} and χ_{III} given, respectively, by Eqs. (C9) and (C10) are introduced from order of magnitude estimates based on the assumptions $(dB/dx)_+ = O(1)$ on measure K

and on ordering the double limit as $K\to 0$ and $\lambda\to\infty$ as given in Clarke and Delale,[19] such that $(dg/dx)_l = O(1)$ on measure K, namely

$$\lambda^3 = O[K^{-3/2}\exp(K^{-1}B_l)], \quad \text{as } K\to 0. \tag{C16}$$

APPENDIX D: ASYMPTOTIC SOLUTION OF THE RATE EQUATION DOWNSTREAM OF THE NORMAL SHOCK IN REGIME IV

Similar to the analysis of Appendices A, B, and C, the asymptotic expression for g downstream of the normal shock in DGZ of this regime takes the form

$$g = R_{\rm IV}^3 + \epsilon_2^{\rm IV} R_{\rm IV}^2 + \epsilon_1^{\rm IV} R_{\rm IV} + \epsilon_0^{\rm IV}, \tag{D1}$$

where $R_{\rm IV}$ satisfies the relaxation rate equation,

$$\frac{dR_{\rm IV}}{d\chi_{\rm IV}} = \hat{\Omega}, \tag{D2}$$

subject to $R_{\rm IV}=0$ at $\chi_{\rm IV}=0$. $\hat{\Omega}=\Omega_2/\Omega_+$. The scaling variables $R_{\rm IV}$ and $\chi_{\rm IV}$ are defined by

$$R_{\rm IV} \equiv \Lambda_{\rm IV} K^{-1/3}\hat{R}(x;K), \tag{D3}$$

$$\chi_{\rm IV} \equiv \Lambda_{\rm IV} K^{-1/3}(x-z) \geqslant 0, \tag{D4}$$

with

$$\Lambda_{\rm IV} \equiv (\sqrt{\pi b_l K})^{1/3}\lambda\Omega_+, \tag{D5}$$

and $\hat{R}$ is given by Eq. (A14) of Appendix A. The coefficients $\epsilon_0^{\rm IV}$, $\epsilon_1^{\rm IV}$, and $\epsilon_2^{\rm IV}$ of Eq. (D1) are defined as

$$\epsilon_0^{\rm IV} \equiv \sqrt{\pi b_l}[(r_l^* + a_l\delta_l)^3 + \tfrac{3}{2}a_l^2(r_l^* + a_l\delta_l)], \tag{D6}$$

$$\epsilon_1^{\rm IV} \equiv 3(\sqrt{\pi b_l})^{2/3}[(r_l^* + a_l\delta_l)^2 + \tfrac{1}{2}a_l^2], \tag{D7}$$

$$\epsilon_2^{\rm IV} \equiv 3(\sqrt{\pi b_l})^{1/3}(r_l^* + a_l\delta_l), \tag{D8}$$

where a_l, b_l, and δ_l are given, respectively, by Eqs. (C2), (C3), and (C5) of Appendix C. From Eqs. (D1) and (D2) and the corresponding equations upstream given in DGZ of Paper I, one can easily verify that the appropriate normal shock relation for dg/dx in this regime is that of the limiting case given by Eq. (8). Finally, we should mention that a simplified analysis of the rate equation in this regime is already available from the work of Clarke and Delale.[7]

[1] C. F. Delale, G. H. Schnerr, and J. Zierep, "Asymptotic solution of transonic nozzle flows with homogeneous condensation. I. Subcritical flows," Phys. Fluids A **5**, 2969 (1993).

[2] G. Jungclaus and O. van Raay, "Berechnung der Strömung in Laval-düsen mit beliebig verteilter Wärmezufuhr," Ing.-Arch. **36**, 226 (1967).

[3] J. Zierep, *Strömungen mit Energiezufuhr* (Braun, Karlsruhe, 1990).

[4] A. A. Pouring, "Thermal choking and condensation in nozzles," Phys. Fluids **8**, 1802 (1965).

[5] D. Barschdorff, "Verlauf der Zustandgrössen und gasdynamischen Zusammenhänge bei der spontanen Kondensation reinen Wasserdampfes in Lavaldüsen," Forsch. Ing. **37**, 146 (1971).

[6] D. Barschdorff and G. A. Fillipov, "Analysis of certain special operating modes of Laval nozzles with local heat supply," Heat Transfer Sov. Res. **2**, 76 (1970).

[7] J. H. Clarke and C. F. Delale, "Supercritical shocks in nozzle flows with nonequilibrium condensation," Phys. Fluids **29**, 1414 (1986).

[8] B. Schmidt, "Theorie und Konstruktion eines Interferometers nach Mach-Zehnder," Dissertation, Technische Hochschule Karlsruhe, 1962.

[9] D. Barschdorff, "Kurzzeitfeuchtemessung und ihre Anwendung bei Kondensationserscheinungen in Lavaldüsen," Mitt. Inst. Strömungslehre Strömungsmaschinen, Heft 6, Universität Karlsruhe, 1967.

[10] F. Mosnier, "Unsteady supersonic flow with heat addition due to condensation," Ph.D. thesis, Yale University, 1976.

[11] P. P. Wegener and F. Mosnier, "Periodic transonic flow with heat addition: New results," Combust. Sci. Technol. **24**, 179 (1981).

[12] C. F. Delale, G. H. Schnerr, and J. Zierep, "The mathematical theory of thermal choking in nozzle flows," Z. Angew. Math. Phys. **44**, 943 (1993).

[13] G. H. Schnerr, "2-D transonic flow with energy supply by homogeneous condensation: Onset condition and 2-D structure of steady Laval nozzle flow," Exp. Fluids **7**, 145 (1989).

[14] H. G. Stever, "Condensation phenomena in high speed flows," in *Fundamentals of Gas Dynamics. High Speed Aerodynamics and Jet Propulsion* (Princeton University Press, Princeton, NJ, 1958), Vol. III.

[15] G. H. Schnerr and U. Dohrmann, "Theoretical and experimental investigation of 2-D diabatic transonic and supersonic flow fields," in *Proceedings of the IUTAM Symposium Transsonicum III*, edited by J. Zierep and H. Oertel (Springer-Verlag, Berlin, 1989), p. 131.

[16] P. A. Blythe and C. J. Shih, "Condensation shocks in nozzle flows," J. Fluid Mech. **76**, 593 (1976).

[17] M. Abramowitz and A. Stegun, *Handbook of Mathematical Functions* (Dover, New York, 1965).

[18] I. S. Gradshteyn and I. M. Ryzhik, *Tables of Integrals, Series and Products* (Academic, New York, 1980).

[19] J. H. Clarke and C. F. Delale, "Nozzle flows with nonequilibrium condensation," Phys. Fluids **29**, 1398 (1986).